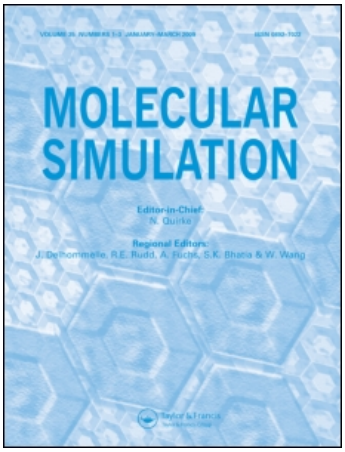

Molecular Simulation
Publication details, including instructions for authors and subscription information:
http://www.informaworld.com/smpp/title~content=t713644482

Molecular investigation of the interactions of trehalose with lipid bilayers of DPPC, DPPE and their mixture

S. Leekumjorn[a]; A. K. Sum[a]
[a] Department of Chemical Engineering, Virginia Polytechnic Institute and State University, Blacksburg 24061, VA, USA

To cite this Article Leekumjorn, S. and Sum, A. K.(2006) 'Molecular investigation of the interactions of trehalose with lipid bilayers of DPPC, DPPE and their mixture', Molecular Simulation, 32: 3, 219 — 230
To link to this Article: DOI: 10.1080/08927020600586565
URL: http://dx.doi.org/10.1080/08927020600586565

Molecular Simulation, Vol. 32, Nos. 3–4, 15 March–April 2006, 219–230

Taylor & Francis
Taylor & Francis Group

Molecular investigation of the interactions of trehalose with lipid bilayers of DPPC, DPPE and their mixture

S. LEEKUMJORN and A. K. SUM*

Department of Chemical Engineering, Virginia Polytechnic Institute and State University, Blacksburg 24061, VA, USA

(Received December 2005; in final form January 2006)

Molecular dynamics simulations were performed to study structural and dynamic properties of fully hydrated pure and mixed bilayers of 1,2-dipalmitoyl-*sn*-glycero-3-phosphocholine (DPPC) and 1,2-dipalmitoyl-*sn*-glycero-3-phosphoethanolamine (DPPE) in the presence of trehalose (5 wt%). Simulations were performed for 50 ns at 350 K and 1 bar in the liquid-crystalline state of the lipid bilayers. At the concentration considered, the effect of trehalose on pure and mixed DPPC/DPPE structure are minimal, with the area per headgroup and lipid tail order parameter unchanged compared to systems without trehalose. Density profiles indicate a larger concentration of trehalose near the interface, suggesting preferential binding of trehalose with the bilayer. Hydrogen bond analysis between trehalose and the bilayers shows that the largest number of interactions occurs with DPPC lipids, whereas the fewest interactions occur in a mixed 1:1 DPPC/DPPE bilayer. The latter is a result of the inter and intramolecular binding of the amine group in DPPE, thus preventing trehalose from hydrogen bonding to the bilayer. For the pure DPPE bilayer, an excess of hydrogen-donors (amine groups) create a competitive hydrogen bonding environment that weakens lipid–lipid interactions and favors hydration of the amine groups, which enhances the binding of trehalose with the bilayer.

Keywords: Molecular dynamics simulations; DPPC; DPPE; Trehalose

1. Introduction

For several decades, the widespread usage of cryoprotectant agents in biological preservation has attracted multidisciplinary research to further understand this phenomena. There have been numerous studies and hypotheses on the effectiveness of these agents based on their chemical properties and their interactions with biological organisms. Naturally occurring stabilizing agents such as disaccharides (e.g. trehalose and sucrose) have been experimentally found to exhibit the most cryo and lyoprotectant activities in animal and plant cells [1,2]. With trehalose acting as a stabilizing agent, cryo and lyoprotection have allowed the preservation of animal cells at extreme conditions above and below normal physiological conditions. The focus of this phenomena has been shown to be the direct interaction of trehalose with the cell membrane, consisted primarily of a phospholipid bilayer. For example, addition of a disaccharide into a liposome suspension significantly prevented encapsulated solution leakage during freezing and freeze-drying [3,4]. Inhibition of cell fusion, phase separation and formation of non-bilayer phases have also been observed in membrane experiments in the presence of trehalose [1,5,6]. Theoretical models and hypotheses have been proposed to explain the mechanism by which trehalose interacts with the phospholipid bilayer to preserve the cell structure and biological function.

In the preferential exclusion model, it is suggested that disaccharides are excluded from the vicinity of the biological structure, thus preserving the hydration shell and maintaining the necessary level of hydration during water deficit conditions [7]. In this case, disaccharides directly interact with water within the solvation shell and behave as an additional protective layer, excluding a portion of water from the surrounding. In the preferential interaction model, several hypotheses has been proposed to explain the direct interaction of disaccharide with the hydrophilic domain of biological structures under harsh conditions, exhibiting protective and stabilizing effects [8]. Three of these hypotheses are: water-replacement [5], water-entrapment [9] and vitrification [10]. In the water-replacement hypothesis, it is suggested that trehalose works as a substitute for water nearby the phospholipid

*Corresponding author. Tel.: + 1-540-231-7869. Fax: + 1-540-231-5022. Email: asum@vt.edu

Molecular Simulation
ISSN 0892-7022 print/ISSN 1029-0435 online © 2006 Taylor & Francis
http://www.tandf.co.uk/journals
DOI: 10.1080/08927020600586565

polar headgroups in the drying process [1,11]. In this case, trehalose forms hydrogen bonds with the phospholipid headgroups, resulting in the stabilization of the membrane structure in the dehydrated state. In the water-entrapment hypothesis, it is argued that, during the drying process, trehalose strongly interacts with both water and phospholipid headgroups causing a slight increase in the hydration near the membrane interface [9,12,13]. Trehalose that comes in contact with the phospholipids provides additional and favorable surface area for water to bind to the hydroxyl groups in trehalose. This is the result of hydrogen bonding between phospholipid and trehalose, and trehalose and water which helps to preserve the membrane structure by maintaining a level of hydration. Finally, in vitrification hypothesis, trehalose acts as a vitrifying agent, protecting the membrane structure through the formation of an amorphous glass in the drying process [10,14–17]. This maintains the original membrane structure and prevents mechanical stress to the membrane under harsh conditions. Within the last decade, a number of experimental studies have linked these hypotheses, indicating that the water-replacement, water-entrapment and vitrification processes are not mutually exclusive processes, but altogether they play a part in the preservation of biological structures [11,14,18,19].

For a better understanding of this preservation mechanism, several investigations of model cell membranes (phospholipid bilayers) in the presence of trehalose have been reported [5,20–24].These studies included a number of analytical methods to probe the interactions between trehalose and the bilayer structure. Crow *et al.* [5] used DSC (differential scanning calorimetry) to measure the phase transition temperature of phospholipid bilayers containing 1,2-dipalmitoyl-*sn*-glycero-3-phosphocholine (DPPC) with and without trehalose. It was found that trehalose caused a significant drop in the phase transition temperature (314 K) from a gel to a liquid-crystalline state of about 30 K. This change was suggested to be due to the replacement of water molecules surrounding the phospholipids by trehalose. To verify this phenomenon, infrared spectroscopy was used to demonstrate hydrogen bonding between the polar headgroups in DPPC and the hydroxyl groups in trehalose. Lee *et al.* [20] used solid-state NMR to monitor the ^{31}P spectra of phospholipid bilayers; their studies indicated less mobility of the phospholipid headgroups upon binding of trehalose. Luzardo *et al.* [21] used FTIR to describe the hydration state of bilayers composing of 1,2-dimyristoyl-*sn*-glycero-3-phosphocholine (DMPC) and trehalose. They determined that three trehalose molecules were able to bind to one DMPC by replacing 11 of 14 water molecules per phospholipid. It was concluded that water replacement occurs at the carbonyl and phosphate groups where the hydroxyl groups of trehalose change the water activity within the phospholipid solvation shell. Lambruschini *et al.* [22] investigated the interaction of trehalose and phospholipid headgroup using Langmuir monolayers. They showed that the critical area corresponding to the surface potential increased in phospholipid–trehalose systems, indicating that trehalose binds to the phospholipid polar headgroups. At high surface pressure, they also demonstrated a strong binding interaction, as trehalose remained intact on the phospholipid headgroups without being expelled from the surface. Ricker *et al.* [23] used FTIR to study the phase behavior of 1,2-dilauroyl-*sn*-glycero-3-phosphocholine (DLPC) and 1,2-distearoyl-d70-*sn*-glycero-3-phosphocholine (DSPCd-70) bilayer mixtures in the presence of trehalose. They observed that the DLPC component of the mixture is strongly fluidized by trehalose while the DSPCd-70 component is not affected when undergoing the drying process. After a heating process, they observed that the phase separation between the phospholipids is maintained, suggesting that trehalose preserves the structure and composition of the phases in microdomains. Recently, Ohtake *et al.* [24] used DSC to investigate the melting temperature of DPPC, 1,2-dipalmitoyl-*sn*-glycero-3-phosphoethanolamine (DPPE) and 1:1 DPPC/DPPE mixtures in the presence and absence of trehalose. They found that trehalose caused the largest decrease in the melting temperature in DPPC, and the smallest decrease in DPPE, suggesting that DPPE exhibits strong interactions with the phospholipids, thus limiting the ability of trehalose to hydrogen bond with the polar headgroups in DPPE.

Several computational studies have also been recently performed on model cell membranes in the presence of trehalose to investigate the mechanism of interaction between phospholipids and trehalose. Chandrasekhar and Gaber [25] performed energy minimization on a phospholipid–trehalose system (without water) and found a slight increase in the area per headgroup for the phospholipid in the presence of trehalose. They also showed that trehalose has favorable conformation to bridge several phospholipids by means of hydrogen bonds. In a similar study, Rudolph *et al.* [26] found that the phospholipid-saccharide interaction energy becomes less stable in the order of trehalose $<$ glucose $<$ sucrose. A more detailed study with molecular simulation was performed by Sum *et al.* [27], Pereira *et al.* [28] and Villarreal *et al.* [29] to investigate the interaction of trehalose with a model cell membrane (DPPC bilayer). The three separate studies reached similar conclusion in that trehalose interacts favorably with the DPPC polar headgroup at the phospholipid–water interface without altering the bilayer structure. At the concentrations studied, no significant changes in the area per headgroup and in the order parameter of lipid tails were observed from the simulations. The water replacement hypothesis was highlighted as a potential mechanism of interaction, where direct hydrogen bonding was observed between trehalose and DPPC, and these interactions were enhanced when the bilayer was subjected to dehydrated conditions.

All the studies of bilayer structures with trehalose thus far have only considered one kind of phospholipid, namely DPPC. However, cell membranes are composed of a range of phospholipids that vary both in the headgroup and fatty

acid composition. In order to obtain a better assessment of the interactions of trehalose with a more realistic bilayer structure, this study presents molecular dynamics simulations for a mixed bilayer of DPPC. DPPE is chosen as the second phospholipid, since the PE headgroup is associated with a wide variety of biological functions including cell division, membrane fusion, vesicle formation, growth, reproduction and motility [30–35]. Moreover, the PE headgroup is found in large concentrations in the inner leaflet of membranes, and it has been determined that the effectiveness of trehalose in protecting biological membranes requires trehalose to be present both in the intra and extracellular environment [4,36–38]. The main difference between DPPE and DPPC is the chemical composition of the headgroups, namely the primary amine group in DPPE functioning as a strong hydrogen donor and the choline group in DPPC providing weak hydrophilic interactions. The aim of this paper is to investigate the interactions between trehalose and pure DPPE and a mixed 1:1 DPPC/DPPE bilayer. The simulations presented here also resolve issues related to the competition of DPPE, DPPC, trehalose and water for hydrogen bonds. We provide a detailed analysis of the structural and dynamic properties of DPPC/DPPE–trehalose systems commonly encountered in biological systems.

2. Simulation Details

Molecular dynamics simulations were performed on systems containing a total of 256 lipid molecules (128 per leaflet) arranged in a bilayer structure. Fully hydrated systems containing DPPC, DPPE and 5 wt% trehalose (lipid-free basis) were studied for the compositions shown in table 1. Figure 1 shows the structure and the assigned numbering considered for the atoms in trehalose (see previous publication for the assigned atom numbers in DPPC and DPPE [39]). Lipid-A, -B and -C were constructed by randomly inserting trehalose molecules into the aqueous region of previously equilibrated pure and mixed lipid bilayer systems (see Leekumjorn and Sum [39] for details). In this work, we refer to these systems without trehalose as Lipid-D, -E, and -F (see table 1).

Table 1. Composition for pure and mixed DPPC/DPPE- trehalose bilayer systems.

System	*DPPC per leaflet*	*DPPE per leaflet*	*Water*	*Trehalose*
Lipid-A	128	0	7225	20
Lipid-B	64	64	7225	20
Lipid-C	0	128	7225	20
Lipid-D*	128	0	7680	0
Lipid-E*	64	64	7680	0
Lipid-F*	0	128	7680	0

A total of 256 lipids were used for all systems. Number of lipids are per leaflet and each leaflet contains the same number of DPPC and DPPE molecules.
*Original lipid compositions before inserting trehalose [39].

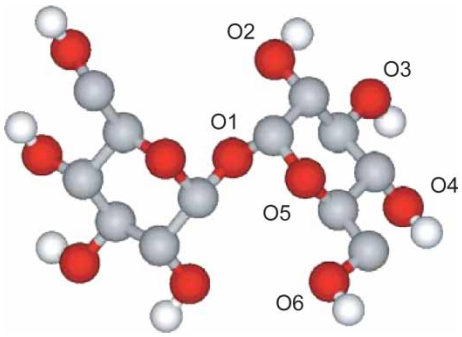

Figure 1. Molecular structures and assigned numbering of atoms in trehalose. Hydrogen, carbon and oxygen atoms are presented by off-white, gray and red spheres, respectively. Hydrogen atoms bound to carbon atoms are not shown. See online version for colour figure.

During the insertion process, overlapping water molecules with trehalose were removed and additional water molecules were subsequently removed to obtain a 5 wt% trehalose concentration. A low trehalose concentration was chosen since, it is in the range of values reported in cryopreservation, lyophilization and other modeled membrane-trehalose studies [3–6]. Figure 2 shows a snapshot of Lipid-B system, a mixed 1:1 DPPC/DPPE bilayer. Note that a uniform distribution of DPPC and DPPE molecules are used for both leaflets.

Intramolecular parameters for bonds, angles, proper dihedral and improper dihedral were consistent with previous studies [40,41]. The Ryckaert–Bellemans potential was used for the torsion potential of the hydrocarbon chains [42]. Non-bonded interactions were described by the parameters from Berger *et al.* [43–45] and partial atomic charges were obtained from Chiu *et al.* [46]. The all atom optimized potentials for liquid simulations (OPLS-AA) force field was used for trehalose [47]. Single point charge (SPC) model was adopted for water [48]. The united-atom representation was used for

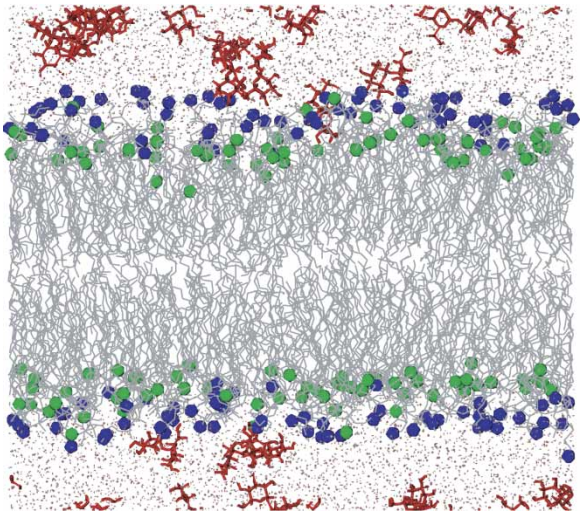

Figure 2. Snapshot of Lipid-C system at 350 K. Colored molecules are DPPC headgroup (blue), DPPE headgroup (green), lipid tails (gray), trehalose (red) and water (pink). See table 1 for additional information. See online version for colour figure.

the methyl/methylene groups in the alkyl chains of both DPPC and DPPE.

Steepest-decent energy minimizations were performed on Lipid-A, -B, and -C, followed by 50 ns simulations. All simulations were performed in the *NPT* ensemble. Temperature and pressure were kept constant at 350 K and 1 bar, respectively (see previous publication for more details on the parameters used in the simulations [39]). All simulations were performed with particle-mesh Ewald (PME) [49,50] to account for the long-range electrostatic correction. Trajectories were collected every 2 ps. All simulations were performed with the GROMACS 3.3-beta software package [51,52] (single-precision mode) in parallel (about 3.2 ns/day in 12 nodes) using Virginia Tech's System X (dual 2.3 GHz Apple Xserve G5) [53].

3. Results and discussion

A number of quantities were analyzed to characterize the effect of trehalose on the properties of pure and mixed bilayers, including: area per headgroup, lipid tail order parameter, mean-squared displacement, density profiles, lipid binding and configuration, hydrogen bonding, and binding and diffusion of trehalose. Results for the lipid systems without trehalose have been reported elsewhere [39] and where appropriate, are shown here for comparison. All simulations were performed at 350 K, which is above the main phase transition from a gel to a liquid-crystalline state. Experimentally, the phase transition for the compositions considered are: 315 K for pure DPPC [54], 329 K for 1:1 DPPC/DPPE, and 337 K for pure DPPE, as reported by Petrov *et al.* [55]. As noted in our previous publication [39], the mixed 1:1 DPPC/DPPE bilayer contained an even number of DPPC and DPPE molecules on each leaflet, a condition necessary in order to obtain a stable system.

The area per headgroup (or lipid), calculated from the cross-sectional area of the simulation boxes (plane along the bilayer interface), for the systems listed in table 1 are shown in figure 3 over the course of the simulation time. The average area per headgroup remains constant throughout the simulation and it is a good measure of the stability of the systems. Also shown in the figure are the results from our previous simulations for the pure and mixed bilayers without trehalose. Table 2 shows the actual numerical averages. Also shown in table are the results for the corresponding lipid system without trehalose [39]. The average values of the area per headgroup for Lipid-A and -C are 0.655 ± 0.005 and $0.522 \pm 0.005\,\mathrm{nm}^2$, respectively. For the DPPC–trehalose system, previous simulations results reported an average area per headgroup of $\sim 0.666\,\mathrm{nm}^2$ at 350 K for 3.4–18.1 wt% trehalose concentration [56], 0.56–$0.58\,\mathrm{nm}^2$ at 325 K for 25.5–51.0 wt% trehalose concentration [28] and $\sim 0.629\,\mathrm{nm}^2$ at 323 K for 13.5 wt% trehalose concentration [29]. For the DPPE–trehalose and mixed 1:1 DPPC/DPPE–trehalose systems, experimental or simulation data are currently unavailable. As seen from the results, the area per headgroup is unchanged by the presence of trehalose, whether the bilayer is composed of DPPC, DPPE or a mixture thereof. In a similar manner as explained previously for DPPC [56], the interactions of trehalose with DPPE and DPPC/DPPE bilayers are only superficial, along the interface through occasional binding to the headgroups, and for this reason, trehalose is unable to deformed the bilayer at low concentrations. Further reasoning is given below.

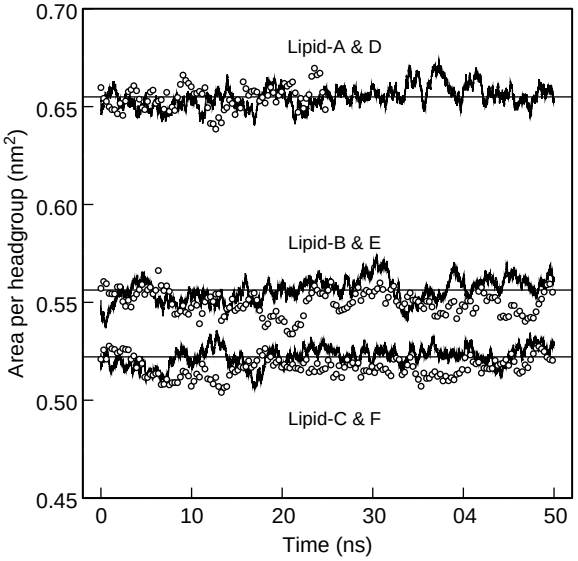

Figure 3. Area per headgroup for the pure and mixed lipid systems over the course of the simulations (solid line). Straight lines show the average area per headgroup for lipid systems containing trehalose. Circles show the area per headgroup for lipid systems without trehalose [39]. See table 1 for additional information.

Figure 4 shows the total density profiles of the bilayer systems along the normal direction to the bilayer surface averaged between 10 and 50 ns. We excluded the first 10 ns in the calculation to eliminate the bias resulting from the unequilibrated system after the insertion of trehalose into the aqueous phase. The interface is the region with the highest density (|1.5–2.5| nm), corresponding to the lipid headgroups and interfacial water. The region (|2.5–4.0| nm) of approximately $1000\,\mathrm{kg/m}^3$ corresponds to the aqueous phase (water and trehalose), and the section with the lowest density at the center of the bilayer structure

Table 2. Calculated equilibrium properties of bilayer systems.

System	*Area per lipid**	D_{DPPC}[†]	D_{DPPE}[†]	$D_{Trehalose}$[†]
Lipid-A	0.655 ± 0.005	0.49 ± 0.1	–	5.27 ± 0.1
Lipid-B	0.556 ± 0.006	0.43 ± 0.1	0.45 ± 0.1	6.05 ± 0.1
Lipid-C	0.522 ± 0.005	–	0.31 ± 0.2	4.81 ± 0.2
Lipid-D[‡]	0.654 ± 0.006	0.79 ± 0.1	–	–
Lipid-E[‡]	0.550 ± 0.006	0.51 ± 0.1	0.48 ± 0.1	–
Lipid-F[‡]	0.517 ± 0.005	–	0.32 ± 0.2	–

D_{DPPC} and D_{DPPE} represent 2D (lateral) diffusion coefficient. $D_{\mathrm{Trehalose}}$ represents 3D diffusion coefficient. All results are for simulations at 350 K.
[*] Values reported in nm^2.
[†] Values reported as $D \times 10^6\,\mathrm{cm}^2/\mathrm{s}$.
[‡] Results from Leekumjorn and Sum [39].

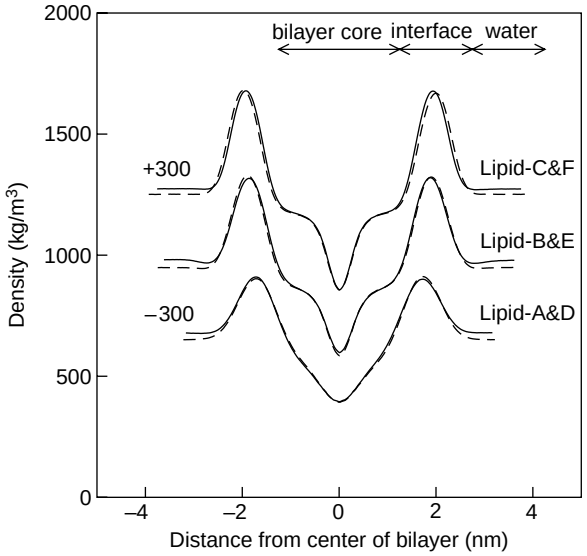

Figure 4. Total density profiles of fully hydrated bilayer systems at 350 K. Solid lines correspond to Lipid-A, -B and -C. Dash lines correspond to previous results from Leekumjorn and Sum [39]. Numbers are the displacement of the profiles, shifted for clarity.

corresponds to the terminal lipid tails. The density profile of Lipid-C compared to -F demonstrates a slight change in the bilayer structure, where the thickness of the bilayer slightly increases (based on the distance between two maximum peaks in the total density profile). Similar feature is observed between Lipid-B and -C in that the total density profile remains relatively unchanged by the presence of trehalose. These observations along with the unchanged area per headgroup suggest that trehalose interacts with the lipid headgroup but does not disrupt the membrane structure.

In order to further quantify the structure of the lipid bilayers and the negligible effect of trehalose on their structure, we analyzed the orientation of the vector formed from the phosphorus to nitrogen atoms (P–N) for both DPPC and DPPE. The intramolecular angle was computed from the angle formed between the P–N vector (phosphorus and nitrogen in the same lipid) and the axis normal to the bilayer surface (z-axis) (see [39] for an illustration of the angle and its meaning). Figure 5 shows the normalized distribution for the angle of the P–N vector for the different lipid systems. The angle distributions for DPPC in Lipid-A and -B are both broad but their maximum values have distinct corresponding angles. In Lipid-A (figure 5a), the wide distribution peaks at about 100 degrees, indicating that the choline groups are exposed to the aqueous phase and unhindered to take any orientation. In Lipid-B (figure 5b), the distribution for the PC groups shifts to lower values, suggesting most of the choline groups are more aligned with the bilayer normal, i.e. more exposed to the aqueous phase. This is caused by closer packing of the lipids in the presence of DPPE (lower area per headgroup). For DPPE in Lipid-B, the majority of the angles for the P–N vector is larger than 90 degrees, indicating that all the amine groups of DPPE in the mixed lipid–trehalose system favorably interact with the lipid oxygen atoms (figure 5b). A bimodal distribution for the P-N angle is observed for DPPE in Lipid-C (figure 5c) showing two preferential sites near the interface (distribution less than 90 degrees) and those near the lipid oxygen atoms (distribution greater than 90 degrees). This demonstrates that there are more H-donors from NH_3 groups in DPPE than available H-acceptors from lipid oxygen atoms, causing the excess H-donors to interact with water at the interface. Comparison of the angle distribution between lipid systems with and without trehalose shows a slight shift in the distributions, thus supporting the idea that trehalose interacts with the membrane but does not alter its structure.

From the individual component density profile of Lipid-A, -B and -C, shown in figure 6a–c, respectively, we observe that trehalose remains in the aqueous phase and does not penetrate into the bilayer core region. Note that the density profiles are shifted so that the center of the plot is in the aqueous phase. In the Lipid-A system (figure 6a), the trehalose density profile is uniform along the aqueous phase, whereas in Lipid-B (figure 6b) and Lipid-C (figure 6c) the density distributions for trehalose are uneven with a slight concentration of trehalose near one

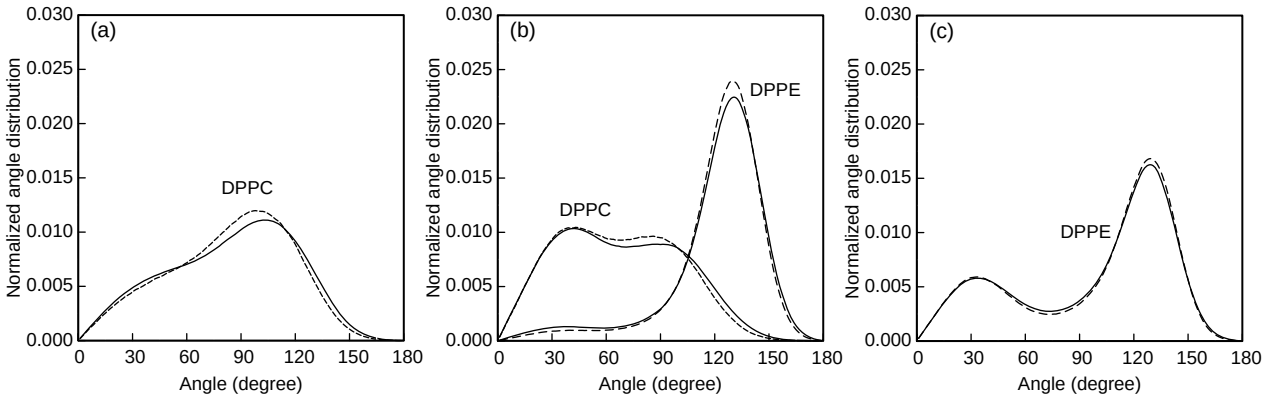

Figure 5. Normalized angle distribution for P–N vector of (a) DPPC in Lipid-A, (b) DPPC and DPPE in Lipid-B and (c) DPPE in Lipid-C. Angle is measured with respect to the normal of the bilayer surface. Dash lines are from previous results of the corresponding bilayer systems without trehalose [39].

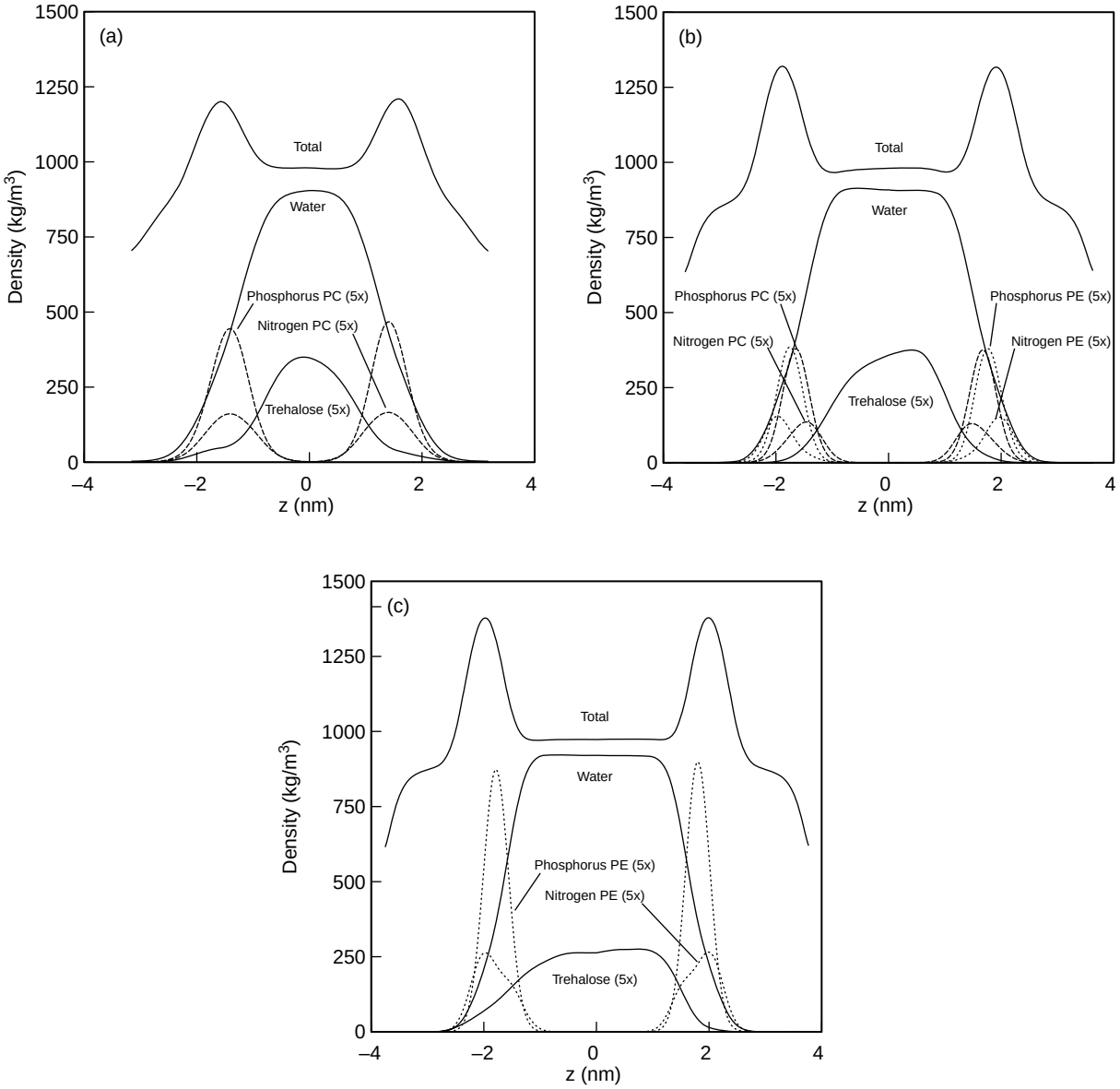

Figure 6. Component density profiles for fully hydrated lipid–trehalose systems at 350 K for (a) pure DPPC, (b) mixed 1:1 DPPC/DPPE and (c) pure DPPE. Number in parenthesis is magnification of profiles.

interface of the membrane, indicating a preferential binding of trehalose with the lipids. As observed in figure 5b and c, the amine group of DPPE is exposed to the aqueous phase at the interface where it can interact strongly with trehalose through hydrogen bonding. For all of the systems considered, trehalose molecules are able to superficially interact with the bilayer interface and hydrogen bond favorably to the phosphate and ester headgroups in the lipid molecules. This is seen from the density profiles extending into the headgroup region as far as the phosphorus density profile. The ester oxygen atoms are the binding sites for the hydroxyl groups in trehalose. The details of this interaction are discussed below.

The effect of trehalose on the bilayer structure was also measured from the lipid tail deuterium order parameter (S_{CD}) [57,39]. Figure 7 shows S_{CD} as a function of the carbon atom along the lipid tails for lipid systems with and without trehalose. The average order parameter of the two lipid tails (*Sn*-1 and -2) are independently reported for DPPC and DPPE. From the properties analyzed thus far, the presence of trehalose at the concentrations studied is seen as minimal and because trehalose is unable to penetrate into the bilayer core, the lipid tail should be minimally affected or should not be affected at all. This is indeed what is observed with the order parameter for the systems with and without trehalose being very similar.

The hydrogen bonding of the NH_3 (amine) group in DPPE provides great insight into the structure of the bilayer and the interactions with trehalose. Figure 8 shows the ensemble average number of hydrogen bonds between NH_3 in DPPE and all oxygen atoms (H-acceptor) in the lipid, trehalose and water, for Lipid-B and -C. The oxygen sites available as H-acceptor are located at the phosphate group (O7, O9, O10, O11), at the two ester groups (O14,

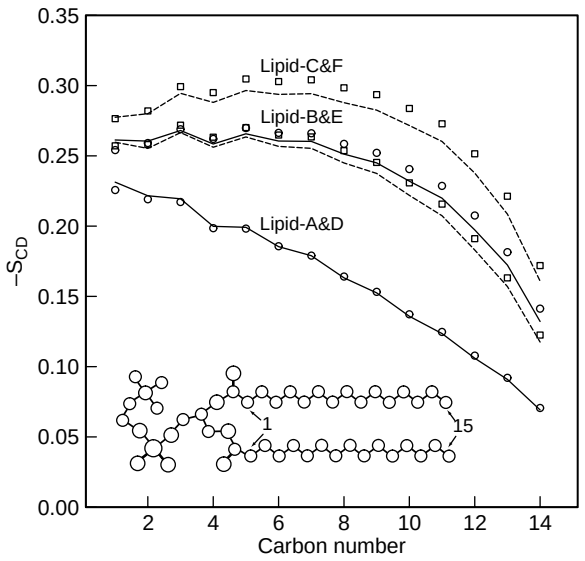

Figure 7. Deuterium order parameter S_{CD} for the phospholipid tails for the pure and mixed bilayer systems containing trehalose at 350 K. The average order parameter for DPPC and DPPE are shown as solid and dashed lines, respectively. Open circles and squares are from previous simulation results of the corresponding bilayer systems without trehalose [39].

O16, O33, O35), trehalose oxygens (O1–O6) and water. Figure 1 shows the pertinent oxygen sites on trehalose and those on the lipid are described in our previous publication [39]. Separate calculations were performed for DPPC and DPPE to differentiate hydrogen bond contributions from each lipid (see figure 8a for intermolecular H-bond between the amine and DPPC lipid oxygen atoms). We also separated contributions resulting from intra and intermolecular hydrogen bonds for DPPE (see figure 8b and c for inter and intramolecular hydrogen bond between DPPE). As discussed previously [39], intramolecular hydrogen bonds are observed for every lipid oxygen and the maximum number of hydrogen bonds is found at O16 for both DPPC and DPPE in Lipid-B and -C (see figure 8a and b). O7 and O16 are the two preferential sites for the NH_3 group in DPPE to form intramolecular hydrogen bonds, which is clearly seen from figure 8c. In figure 8d, hydrogen bonding is observed between the amine and all of the trehalose oxygen atoms, although the binding to some sites can be considered negligible (e.g. hydrogen bonding between NH_3 and O1 of trehalose for Lipid-B and -C is approximately zero). A summary of the average number of hydrogen bonds between the NH_3 group of DPPE and various hydrogen acceptors from water, lipid and trehalose is shown in table 3. The total average number of hydrogen bonds per NH_3 is about 2.74–2.75 (see last row of table 3), independent of the DPPE concentration (this value is expected since there are three H-donors per NH_3). Moreover, it is interesting to see that the total number of hydrogen bonds from the amine group in DPPE is also unaffected by trehalose. In the presence of trehalose, the amine group is able to hydrogen bond with trehalose, which results in a decrease of inter and intramolecular hydrogen bonds between lipids and, consequently, an increase in the number of hydrogen bonds with water. This is shown in table 3 for Lipid-B in comparison to Lipid-E where the number of hydrogen bonds between NH_3 and water per NH_3 increases from 0.439 to 0.557, and the number of inter and intramolecular hydrogen bonds decreases from 0.815 to 0.783 and 1.495 to 1.406, respectively. A similar trend is observed for Lipid-C in comparison to Lipid-F.

From table 3, we also see that the total number of hydrogen bonds per NH_3 (ensemble average) between NH_3 and all trehalose oxygen atoms significantly increased from Lipid-B to -C (approximately 0.004–0.010). The large difference in value demonstrates a preferential binding of trehalose to the amine group in DPPE in Lipid-C. This is expected because the amine group is more exposed in the interface in Lipid-C than in Lipid-B, as observed from the normalized P–N angle distribution previously calculated (see figure 5). As discussed previously [39], this was explained by the fact that there are more H-donors than available H-acceptors as the DPPE concentration increases, resulting in a competition between lipid oxygen atoms and water for hydrogen bonds with the NH_3 groups. From these results, we conclude that hydrogen bonds are formed between NH_3 and trehalose oxygen atoms near the interface in Lipid-C. However, due to the preferential binding of NH_3 to lipid oxygen atoms in Lipid-B, interactions with trehalose are less likely to occur.

A hydrogen bond analysis was also performed to investigate the binding of trehalose as H-donor to other H-acceptors (lipid oxygen atoms). For this analysis, the H-donors are the hydroxyl (OH) groups in trehalose denoted by O2–O6 (see figure 1). Note that trehalose has two glucose rings with the same hydroxyl groups on each ring. Instead of calculating the ensemble average of hydrogen bonds between the OH groups and lipid oxygen atoms, which is relatively small in number, we determined the number of hydrogen bond contacts between these two groups over the course of the simulations, as shown in table 4. Lipid-A shows the largest number of contacts (21.7×10^4). This is expected because the amine groups in Lipid-B and C form inter and intramolecular hydrogen bonds with lipid oxygen atoms, thus preventing trehalose of binding to those same sites. The values calculated are 13.8×10^4 contacts (the sum of DPPC and DPPE) and 16.4×10^4 contacts for Lipid-B and -C, respectively. Based on the number of contacts from Lipid-A, trehalose interacts with lipid oxygen atoms by replacing water molecules, supporting the water-replacement hypothesis. From this analysis, we would expect that Lipid-C would have the least amount of hydrogen bond contacts because of the highest concentration of amine groups that prevent trehalose to interact freely with lipid oxygen atoms; however, this is not the case. This can be explained by two factors. First, the P–N angle distribution (figure 5) and the trehalose density profile (figure 6) suggest that a significant amount of amine groups in DPPE are exposed

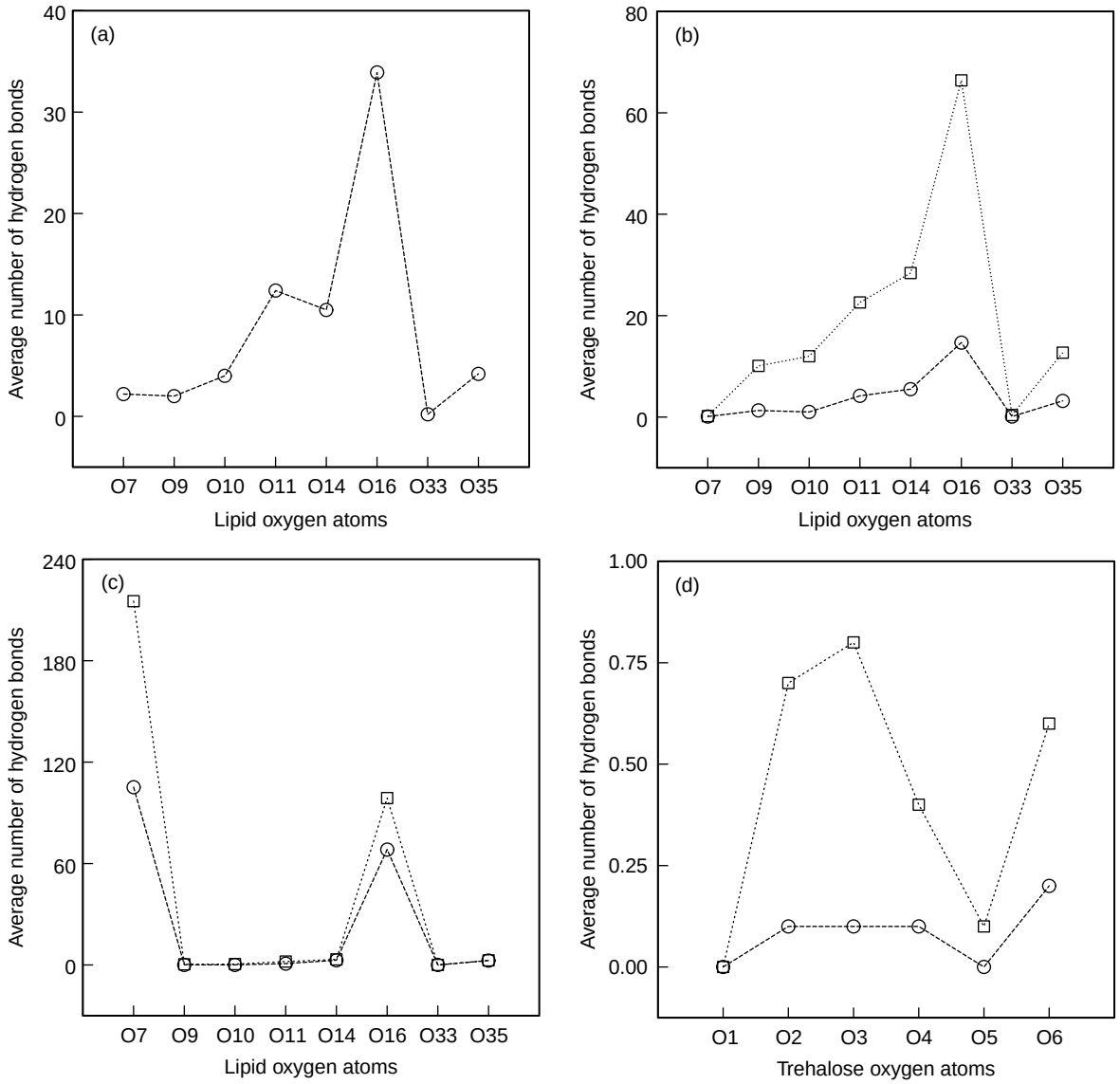

Figure 8. Average number of (a) hydrogen bond between DPPE amine group and DPPC oxygen atoms, (b) intermolecular hydrogen bond between DPPE amine group and neighboring DPPE oxygen atoms, (c) intramolecular hydrogen bond between DPPE amine group and their oxygen atoms and (d) hydrogen bond between DPPE amine group and trehalose oxygen atoms. Circles and square are the calculated values for Lipid-B and -C, respectively. Dot and dash lines are shown as guide.

to the aqueous phase in Lipid-C compared to Lipid-B. These amine groups are at the interface and they can easily hydrogen bond to the hydroxyl groups in trehalose. Consequently, at the interface, the hydroxyl groups are then in the range to form hydrogen bonds with lipid oxygen atoms. Note that for every trehalose molecule that comes in contact with an amine group, there are a total of eight hydroxyl groups that can potentially form hydrogen bonds with lipid oxygen atoms. Second, due to the competition between excess H-donors and H-acceptors in lipid oxygen atoms or water as described in details in our previous publication [39], we observe a slight increase in the hydration of the amine group of DPPE in Lipid-C, resulting in a reduction of inter and intramolecular hydrogen bond between lipids. This results in a greater increase in the number of hydrogen bond contacts of trehalose with lipid oxygen atoms in Lipid-C than in Lipid-B.

Table 3. Average number of hydrogen bonds between NH_3 group of DPPE and H-acceptors from water, lipid oxygen atoms and trehalose oxygen atoms.

	Lipid-B	*Lipid-E**	*Lipid-C*	*Lipid-F**
H-bond to H_2O/NH_3	0.557	0.439	0.875	0.815
H-bond to trehalose/NH_3	0.004	–	0.010	–
Lipid intra H-bond/NH_3	1.406	1.495	1.261	1.318
Lipid inter H-bond/NH_3	0.783	0.816	0.597	0.603
Total H-bonds/NH_3	2.750	2.750	2.743	2.736

Average number of inter and intramolecular hydrogen bonds are calculated separately for the lipids. Note that all values are reported per NH_3.
*Results from Leekumjorn and Sum [39].

Figure 9 shows the mean-squared displacement (MSD) of the lipid molecules for all lipid-trehalose systems. Previous MSD of DPPC, DPPE, 1:1 DPPC/DPPE bilayers without trehalose [39] are also shown for comparison.

Table 4. Approximate number of hydrogen bond contact between trehalose hydroxyl groups and lipid oxygen atoms over the course of 50 ns simulations.

Lipid	*Lipid-A**	*Lipid-B**	*Lipid-B*†	*Lipid-C*†
O7	2.4	1.1	0.052	0.20
O9	5.1	2.2	1.9	6.1
O10	4.9	2.1	1.3	4.6
O11	1.7	0.62	0.56	2.0
O14	1.9	0.51	0.071	0.87
O16	3.2	1.4	0.38	1.1
O33	0.15	0.026	0.012	0.053
O35	2.4	1.1	0.50	1.5
Total	21.7	9.0	4.8	16.4
Trehalose	Lipid-A*	Lipid-B*	Lipid-B†	Lipid-C†
O2	4.3	2.0	0.49	3.0
O3	5.8	2.5	1.2	4.6
O4	5.8	2.6	1.2	4.6
O6	5.8	1.8	1.9	4.2
Total	21.7	9.0	4.8	16.4

Individual contact points are independently reported for DPPC and DPPE in the mixed lipid systems. Contacts are counted only for trajectories saved every 2 ps. Numbers are reported in $\times 10^4$.
*Interaction between DPPC and trehalose.
† Interaction between DPPE and trehalose.

Although the total simulation time is not the same for Lipid-A (50 ns) and Lipid-D (25 ns), it is still evident that the displacement of the lipids is slightly reduced in the systems containing trehalose. This suggests that trehalose interacts with the lipid molecules and their dynamics change due to this binding. For Lipid-C, in comparison to Lipid-F, it is also seen that trehalose reduces the movement of lipid molecules. Minor differences in the MSD for Lipid-B and -E suggest weaker interactions between trehalose and lipid molecules. The calculated 2D diffusion coefficients for the lipids (shown in table 2) range from $0.31 \pm 0.2 \times 10^{-6}$ to $0.49 \pm 0.1 \times 10^{-6}\,cm^2/s$. For the DPPC-trehalose system, the estimated values for the lateral diffusion coefficient of lipids are $0.31–0.37 \times 10^{-6}\,cm^2/s$ at 325 K [28] and $\sim 0.33 \times 10^{-6}\,cm^2/s$ at 350 K [56], which are also in good agreement with the current results. Due to the large uncertainty in determining the diffusion coefficients by fitting a line (slope = 1) to the curves in figure 9, we imposed a larger error estimate in the value for Lipid-C. This reflects the long time required for the lipid molecules to reach a diffusive regime. The diffusion coefficients of trehalose, also shown in table 2, range from $5.27 \pm 0.1 \times 10^{-6}\,cm^2/s$ in DPPC–trehalose to $4.81 \pm 0.2 \times 10^{-6}\,cm^2/s$ in DPPE–trehalose at 350 K. These values are comparable to those obtained from previous DPPC–trehalose simulations of $0.8–3.5 \times 10^{-6}\,cm^2/s$ for 3.40–18.1 wt% trehalose at 350 K [56], $\sim 2.5 \times 10^{-6}\,cm^2/s$ for 25.5–51.0 wt% trehalose at 325 K [28], and from NMR measurements of trehalose in aqueous solutions of $10.1–15.6 \times 10^{-6}\,cm^2/s$ for 3.40–18.1 wt% trehalose at 358 K [58]. The diffusion coefficient of trehalose is slightly lower in Lipid-C, which is consistent with the argument given that trehalose binds to the PE headgroups. For Lipid-B, the diffusion coefficient is the highest, demonstrating that trehalose remains in the aqueous phase. This again is consistent with our current results in which the amine group preferentially binds to lipid oxygen atoms, thus preventing trehalose from binding to those sites.

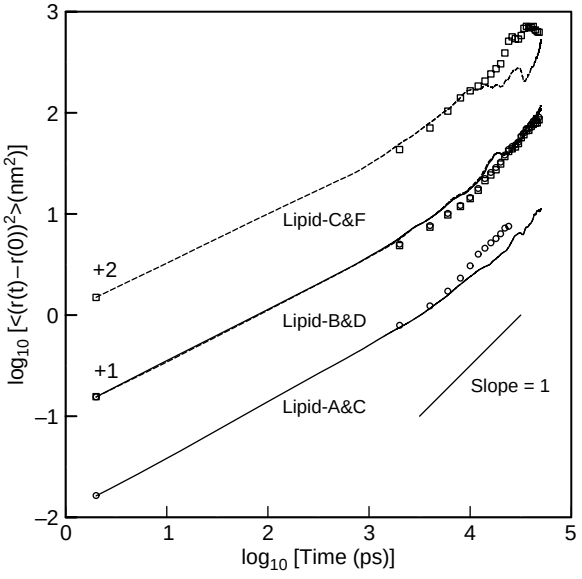

Figure 9. Mean-squared displacement for DPPC and DPPE. Solid and dash lines represent the displacement of PC and PE lipids, respectively, in the lipid systems containing trehalose. Circles and squares are the corresponding results without trehalose from Leekumjorn and Sum [39]. Short solid line has unity slope. Note that curves are displaced for clarity.

To summarize the properties of trehalose in the pure and mixed DPPC/DPPE bilayers, we monitored the dynamics of trehalose from the trajectories over the length of the simulations. Here, we selected one trehalose molecule (represented by the position of O1—see figure 1) from each of Lipid-A, -B and -C, and investigated its interaction with the lipid oxygen atoms, as shown in figure 10a–c, respectively (trajectories shown are with respect to the z direction only). From the figures, it is clear that trehalose is randomly interacting with the membrane interface. Figure 10a and c show close contact of trehalose with the bilayer as the trajectories of trehalose overlap the phosphorus layer at certain times. These contacts are not as pronounced in figure 10b. This re-affirms our findings discussed earlier that the average number of hydrogen bond contacts is the least in Lipid-B. Further analysis of the data provided the hydrogen bond pairs which are responsible for each contact between trehalose and lipid molecules, as shown in figure 10d–f. The hydroxyl groups in trehalose are assumed as H-donors and lipid oxygen atoms as H-acceptors. The plots show the interaction of H-donors with lipid oxygen atoms, denoted by O7, O9–O11, O14, O16, O33 and O35 for DPPC and O7E, O9E–O11E, O14E, O16E, O33E and O35E for DPPE. Comparison of the trajectories plots in the top and bottom rows indicate the times when trehalose binds to the headgroups. For example, figure 10c and f correspond to the trajectory of a trehalose molecule and its binding to the lipids. In this case, trehalose predominantly binds to the phosphate

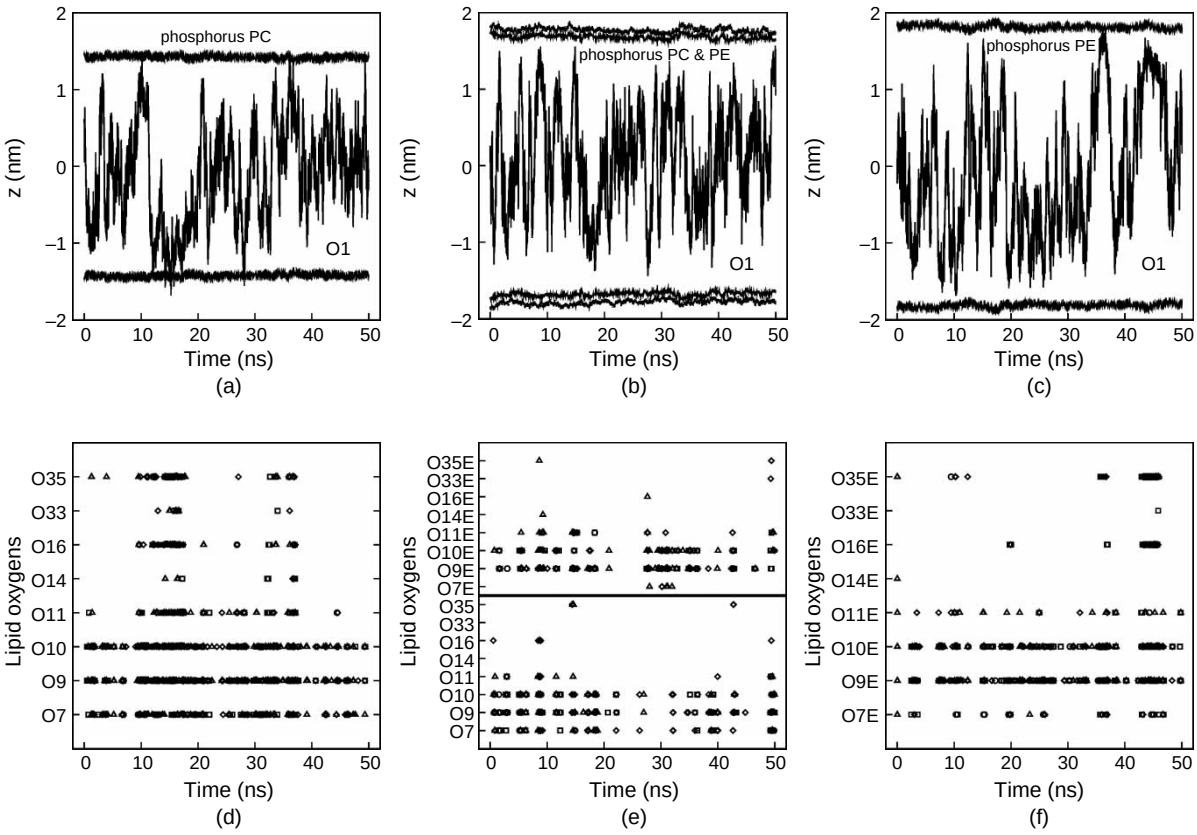

Figure 10. Dynamics of one selected trehalose molecule represented by the position of central oxygen atom (O1) from (a) Lipid-A, (b) Lipid-B and (c) Lipid-C. Corresponding hydrogen bond interaction between the hydroxyl groups of the selected trehalose molecule and lipid oxygen atoms are shown for (d) Lipid-A, (e) Lipid-B and (f) Lipid-C. The hydroxyl groups are O2 (circles), O3 (squares), O4 (diamonds) and O6 (triangles). The average position of phosphorus atoms illustrates the location of bilayer interface. The position $z = 0$ corresponds to middle of aqueous phase. In Figure 10b, the average position of the phosphorus atoms in DPPC and DPPE are independently reported for clarity.

oxygen atoms, while very few interactions occur with the ester groups. On the other hand, the interactions of trehalose with DPPC (figure 10a and d) show that the ester groups are more exposed and more accessible to bind with trehalose, as previously reported [56]. Even though the binding of trehalose with DPPE is stronger than with DPPC, the interactions are more superficial along the interface, that is, there are few interactions of trehalose with the ester headgroups. As such, there is a slight increase in the hydration of the headgroups, since trehalose does not replace as much water as in the case with DPPC.

4. Conclusions

We have presented a systematic simulation study of pure and mixed lipid bilayers of DPPC and DPPE with trehalose. Results indicate that the area per headgroup remains relatively constant for the bilayer systems at 350 K. Total density profiles of all bilayer systems remain relatively unchanged by the presence of trehalose. Preferential binding of trehalose with the lipid systems containing DPPE is observed from the trehalose density profiles where the distributions of trehalose are uneven with a slight concentration of trehalose near one interface of the membrane. From the density profiles, trehalose superficially interacts with the bilayers interface and favorably hydrogen bonds to the phosphate and ester headgroups. Trehalose is unable to penetrate through the interface to the bilayer core, and as a result, the effect of trehalose on the lipid tails is minimal.

With increasing DPPE concentration, the total number of hydrogen bonds from the amine group of DPPE remains unaffected by trehalose as the contribution of hydrogen bonds shift from lipids (inter and intramolecular hydrogen bond) to water and trehalose. A large increase in the binding of trehalose is observed in the lipid systems with higher DPPE concentration. Trehalose can only bind to the amine groups that are exposed to the aqueous phase. The amine group in DPPE preferentially binds to phosphate and ester oxygen atoms through intra or intermolecular hydrogen bonds. Because there are more H-donors than available H-acceptors as the DPPE concentration increases, the excess H-donors create a competitive hydrogen bonding environment that weaken lipid–lipid interactions and simultaneously allow amine groups to become more hydrated. This provides a more favorable condition for trehalose to bind to the lipids.

A hydrogen bond analysis between the hydroxyl groups of trehalose and lipid oxygen atoms shows that the largest number of hydrogen bond contacts in the pure DPPC

bilayer, whereas the mixed 1:1 DPPC/DPPE bilayer shows the least amount of hydrogen bond contacts compared to the pure DPPE bilayer. The diffusion coefficient of trehalose calculated from the mean-squared displacement supports this argument, being the lowest in the pure DPPE bilayer (a large number of amine groups superficially bind to trehalose at the interface). In addition, due to competitive hydrogen bonding environment of the amine groups in pure DPPE bilayer, inter and intramolecular hydrogen bonds between lipids are weakened, creating more suitable conditions for trehalose (hydroxyl groups) to bind to lipid oxygen atoms. However, the same conditions are not true in the mixed 1:1 DPPC/DPPE system. From a different standpoint, the strong interaction of DPPE with neighboring lipids also helps to maintain the membrane integrity, creating a self-preserving mechanism under low hydration conditions. This may help to explain the high survival rate of bacteria (contains as much as about 70–80% PE in *Escherichia coli* [59]) under harsh conditions.

From the trajectory analysis, we see that trehalose is free to diffuse in the aqueous phase and occasionally binds to the bilayer, with multiple lipid–trehalose interaction sites often involved. The binding of trehalose to the bilayer discredits the preferential exclusion model as a major mechanism by which trehalose preserves cells. All bilayer systems considered here are fully hydrated, a condition that may reduce the effectiveness or change the biological properties of trehalose compared to a more dry state. The interactions between trehalose and the bilayer are apparent from the hydrogen bond analysis and the dynamic trajectories, and these evidences support the preferential interaction model, even at low trehalose concentrations.

Acknowledgements

The computational resources were provided by Virginia Tech Terascale Computing Facility (System X).

References

[1] J.H. Crowe, L.M. Crowe, J.F. Carpenter, C.A. Wistrom. Stabilization of dry phospholipid bilayers and proteins by sugars. *Biochem. J.*, **242**, 1 (1987).

[2] J.H. Crowe, L.M. Crowe, A.E. Oliver, N. Tsvetkova, W. Wolkers, F. Tablin. The trehalose myth revisited: introduction to a symposium on stabilization of cells in the dry state. *Cryobiology*, **43**, 89 (2001).

[3] T.D. Madden, M.B. Bally, M.J. Hope, P.R. Cullis, H.P. Schieren, A.S. Janoff. Protection of large unilamellar vesicles by trehalose during dehydration: retention of vesicle contents. *BBA-Biomembranes*, **817**, 67 (1985).

[4] C. Womersley, P.S. Uster, A.S. Rudolph, J.H. Crowe. Inhibition of dehydration-induced fusion between liposomal membranes by carbohydrates as measured by fluorescence energy-transfer. *Cryobiology*, **23**, 245 (1986).

[5] J.H. Crowe, L.M. Crowe, D. Chapman. Preservation of membranes in anhydrobiotic organisms: the role of trehalose. *Science*, **223**, 701 (1984).

[6] F.A. Hoekstra, W.F. Wolkers, J. Buitink, E.A. Golovina, J.H. Crowe, L.M. Crowe. Membrane stabilization in the dry state. *Comp. Biochem. Phys. A*, **117**, 335 (1997).

[7] T. Arakawa, S.N. Timasheff. The stabilization of proteins by osmolytes. *Biophys. J.*, **47**, 411 (1985).

[8] B. Schobert. Is there an osmotic regulatory mechanism in algae and higher plants? *J. Theor. Biol.*, **68**, 17 (1977).

[9] P.S. Belton, A.M. Gil IR and Raman Spectroscopic studies of the interaction of trehalose with hen egg white lysozyme. *Biopolymers*, **34**, 957 (1994).

[10] W.Q. Sun, A.C. Leopold. Glassy state and seed storage stability: a viability equation analysis. *Ann. Bot.-Lond.*, **74**, 601 (1994).

[11] J.F. Carpenter, S.J. Prestrelski, T.J. Anchordoguy, T. Arakawa. Interactions of stabilizers with proteins during freezing and drying. *ACS Sym. Ser.*, **567**, 134 (1994).

[12] G. Cottone, G. Ciccotti, L. Cordone. Protein–trehalose–water structures in trehalose coated carboxy-myoglobin. *J. Chem. Phys.*, **117**, 9862 (2002).

[13] R.D. Lins, C.S. Pereira, P.H. Hünenberger. Trehalose–protein interaction in aqueous solution. *Proteins*, **55**, 177 (2004).

[14] W.Q. Sun, A.C. Leopold. Cytoplasmic vitrification acid survival of anhydrobiotic organisms. *Comp. Biochem. Phys. A*, **117**, 327 (1997).

[15] W.Q. Sun, T.C. Irving, A.C. Leopold. The role of sugar. Vitrification and membrane phase transition in seed desiccation tolerance. *Physiol. Plantarum*, **90**, 621 (1994).

[16] W.Q. Sun, A.C. Leopold, L.M. Crowe, J.H. Crowe. Stability of dry liposomes in sugar glasses. *Biophys. J.*, **70**, 1769 (1996).

[17] R.J. Williams, A.C. Leopold. The glassy state in corn embryos. *Plant Physiol.*, **89**, 977 (1989).

[18] J.S. Clegg. Cryptobiosis–A peculiar state of biological organization. *Comp. Biochem. Phys. B*, **128**, 613 (2001).

[19] L.M. Crowe. Lessons from nature: the role of sugars in anhydrobiosis. *Comp. Biochem. Phys. A*, **131**, 505 (2002).

[20] C.W. Lee, J.S. Waugh, R.G. Griffin. Solid-state NMR study of trehalose/1,2-dipalmitoyl-sn-phosphatidylcholine interactions. *Biochemistry*, **25**, 3737 (1986).

[21] M.C. Luzardo, F. Amalfa, A.M. NÛnez, S. Díaz, A.C. Biondi de Lopez, E.A. Disalvo. Effect of trehalose and sucrose on the hydration and dipole potential of lipid bilayers. *Biophys. J.*, **78**, 2452 (2000).

[22] C. Lambruschini, N. Relini, A. Ridi, L. Cordone, A. Gliozzi. Trehalose interacts with phospholipid polar heads in Langmuir monolayers. *Langmuir*, **16**, 5467 (2000).

[23] J.V. Ricker, N.M. Tsvetkova, W.F. Wolkers, C. Leidy, F. Tablin, M. Longo, J.H. Crowe. Trehalose maintains phase separation in an air-dried binary lipid mixture. *Biophys. J.*, **84**, 3045 (2003).

[24] S. Ohtake, C. Schebor, S.P. Palecek, J.J. de Pablo. Phase behavior of freeze-dried phospholipid–cholesterol mixtures stabilized with trehalose. *BBA-Biomembranes*, **1713**, 57 (2005).

[25] I. Chandrasekhar, B.P. Gaber. Stabilization of the bio-membrane by small molecules: interaction of trehalose with the phospholipid bilayer. *J. Biomol. Struct. Dyn.*, **5**, 1163 (1988).

[26] B.R. Rudolph, I. Chandrasekhar, B.P. Gaber, M. Nagumo. Molecular modeling of saccharide–lipid interactions. *Chem. Phys. Lipids*, **53**, 243 (1990).

[27] A.K. Sum, J.J. de Pablo. Molecular simulation study on the influence of dimethylsulfoxide on the structure of phospholipid bilayers. *Biophys. J.*, **85**, 3636 (2003).

[28] C.S. Pereira, R.D. Lins, I. Chandrasekhar, L.C.G. Freitas, P.H. Hünenberger. Interaction of the disaccharide trehalose with a phospholipid bilayer: a molecular dynamics study. *Biophys. J.*, **86**, 2273 (2004).

[29] M.A. Villarreal, S.B. Díaz, E.A. Disalvo, G.G. Montich. Molecular dynamics simulation study of the interaction of trehalose with lipid membranes. *Langmuir*, **20**, 7844 (2004).

[30] K. Emoto, T. Kobayashi, A. Yamaji, H. Aizawa, I. Yahara, K. Inoue, M. Umeda. Redistribution of phosphatidylethanolamine at the cleavage furrow of dividing cells during cytokinesis. *Proc. Natl Acad. Sci. USA*, **93**, 12867 (1996).

[31] R. Birner, M. Bürgermeister, R. Schneiter, G. Daum. Roles of phosphatidylethanolamine and of its several biosynthetic pathways in *Saccharomyces cerevisiae*. *Mol. Biol. Cell*, **12**, 997 (2001).

[32] R. Jahn, H. Grubmüller. Membrane fusion. *Curr. Opin. Cell. Biol.*, **14**, 488 (2002).

[33] M.K. Storey, K.L. Clay, T. Kutateladze, R.C. Murphy, M. Overduin, D.R. Voelker. Phosphatidylethanolamine has an essential role in

Saccharomyces cerevisiae that is independent of its ability to form hexagonal phase structures. *J. Biol. Chem.*, **276**, 48539 (2001).
[34] P. Martínez, A. Morros. Membrane lipid dynamics during human sperm capacitation. *Front. Biosci.*, **1**, d103 (1996).
[35] D.B. Kearns, J. Robinson, L.J. Shimkets. *Pseudomonas aeruginosa* exhibits directed twitching motility up phosphatidylethanolamine gradients. *J. Bacteriol.*, **183**, 763 (2001).
[36] L.M. Crowe, J.H. Crowe, A. Rudolph, C. Womersley, L. Appel. Preservation of freeze-dried liposomes by trehalose. *Arch. Biochem. Biophys.*, **242**, 240 (1985).
[37] E.C.A. Eleutherio, P.S. de Araujo, A.D. Panek. Role of the trehalose carrier in dehydration resistance of *Saccharomyces cerevisiae*. *BBA-Gen. Subjects*, **1156**, 263 (1993).
[38] T. Chen, J.P. Acker, A. Eroglu, S. Cheley, H. Bayley, A. Fowler, M.L. Toner. Beneficial effect of intracellular trehalose on the membrane integrity of dried mammalian cells. *Cryobiology*, **43**, 168 (2001).
[39] S. Leekumjorn, A.K. Sum. Molecular simulation study of structural and dynamic properties of mixed DPPC/DPPE bilayers. *Biophys. J.*, (2006) in press.
[40] E. Egberts, S.J. Marrink, H.J.C. Berendsen. Molecular dynamics simulation of a phospholipid membrane. *Eur. Biophys. J.*, **22**, 423 (1994).
[41] W.F. van Gunsteren, S.R. Billeter, A.A. Eising, P.H. Hünenberger, P. Krüger, A.E. Mark, W.R.P. Scott, I.G. Tironi. *Biomolecular simulation: the GROMOS96 manual and user guide*, vdf Hochschuleverlag AG an der ETH Zürich, Zürich, Switzerland (1996).
[42] J.P. Ryckaert, A. Bellemans. Molecular dynamics of liquid normal-butane near its boiling-point. *Chem. Phys. Lett.*, **30**, 123 (1975).
[43] O. Berger, O. Edholm, F. Jähnig. Molecular dynamics simulations of a fluid bilayer of dipalmitoylphosphatidylcholine at full hydration, constant pressure, and constant temperature. *Biophys. J.*, **72**, 2002 (1997).
[44] W.L. Jorgensen, J. Tirado-Rives. The OPLS potential function for proteins. Energy minimizations for crystals of cyclic peptides and crambin. *J. Am. Chem. Soc.*, **110**, 1657 (1988).
[45] J.W. Essex, M.M. Hann, W.G. Richards. Molecular dynamics simulation of a hydrated phospholipid-bilayer. *Philos. Trans. R. Soc. B*, **344**, 239 (1994).
[46] S.W. Chiu, M. Clark, V. Balaji, S. Subramaniam, H.L. Scott, E. Jakobsson. Incorporation of surface tension into molecular dynamics simulation of an interface: a fluid phase lipid bilayer membrane. *Biophys. J.*, **69**, 1230 (1995).
[47] W. Damm, A. Frontera, J. TiradoRives, W.L. Jorgensen. OPLS all-atom force field for carbohydrates. *J. Comput. Chem.*, **18**, 1955 (1997).
[48] H.J.C. Berendsen, J.P.M. Postma, W. van Gunsteren, J. Hermans. *Intermolecular Forces*, Reidel, Dordrecht, The Netherlands (1981).
[49] T. Darden, D. York, L. Pedersen. Particle mesh Ewald: an $N\log(N)$ method for Ewald sums in large systems. *J. Chem. Phys.*, **98**, 10089 (1993).
[50] U. Essman, L. Perera, M.L. Berkowitz, T. Darden, H. Lee, L.G. Pedersen. A smooth particle mesh Ewald method. *J. Chem. Phys.*, **103**, 8577 (1995).
[51] H.J.C. Berendsen, D. van der Spoel, R. van Drunen. GROMACS: a message-passing parallel molecular dynamics implementation. *Comput. Phys. Commun.*, **91**, 43 (1995).
[52] E. Lindahl, B. Hess, D. van der Spoel. GROMACS 3.0: a package for molecular simulation and trajectory analysis. *J. Mol. Model.*, **7**, 306 (2001).
[53] Virginia Tech. http://www.tcf.vt.edu (Terascale Computing Facility).
[54] M.J. Janiak, D.M. Small, G.G. Shipley. Nature of the thermal pretransition of synthetic phospholipids: dimyristolyl- and dipalmitoyllecithin. *Biochemistry*, **15**, 4575 (1976).
[55] A.G. Petrov, K. Gawrisch, G. Brezesinski, G. Klose, A. Möps. Optical detection of phase transitions in simple and mixed lipid-water phases. *BBA-Biomembranes*, **690**, 1 (1982).
[56] A.K. Sum, R. Faller, J.J. de Pablo. Molecular simulation study of phospholipid bilayers and insights of the interactions with disaccharides. *Biophys. J.*, **85**, 2830 (2003).
[57] D.P. Tieleman, S.J. Marrink, H.J.C. Berendsen. A computer perspective of membranes: molecular dynamics studies of lipid bilayer systems. *BBA-Biomembranes*, **1331**, 235 (1997).
[58] N. Ekdawi-Sever, J.J. de Pablo, E. Feick, E. von Meerwall. Diffusion of sucrose and α,α-trehalose in aqueous solutions. *J. Phys. Chem. A*, **107**, 936 (2003).
[59] W. Dowhan. Molecular basis for membrane phospholipid diversity: why are there so many lipids? *Annu. Rev. Biochem.*, **66**, 199 (1997).